CHEMISTRY
A EUROPEAN JOURNAL

ChemPubSoc
Europe

DOI: 10.1002/chem.201204342

VIP

Hydroxypalladation Precedes the Rate-Determining Step in the Wacker Oxidation of Ethene

Venkataramana Imandi, Sooraj Kunnikuruvan, and Nisanth N. Nair*[a]

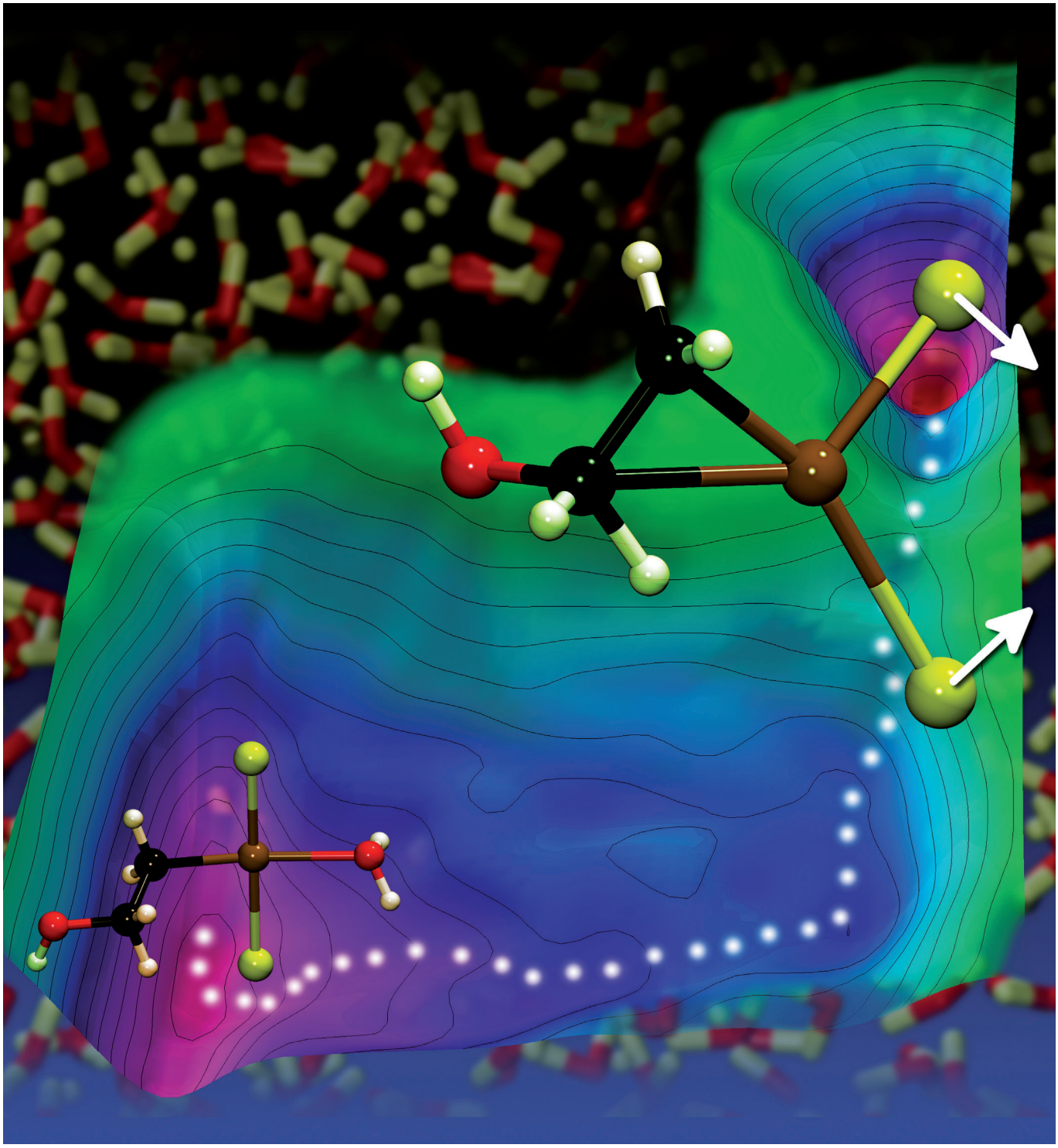

Abstract: The complete reaction mechanism and kinetics of the Wacker oxidation of ethene in water under low [Cl^-], [Pd^{II}], and [Cu^{II}] conditions are investigated in this work by using ab initio molecular dynamics. These extensive simulations shed light on the molecular details of the associated individual steps, along two different reaction routes, starting from a series of ligand-exchange processes in the catalyst precursor $PdCl_4^{2-}$ to the final aldehyde-formation step and the reduction of Pd^{II}. Herein, we report that hydroxylpalladation is not the rate-determining step and is, in fact, in equilibrium. The newly proposed rate-determining step involves isomerization and follows the hydroxypalladation step. The mechanism proposed herein is shown to be in excellent agreement with the experimentally observed rate law and rate. Moreover, this mechanism is in consensus with the observed kinetic isotope effects. This report further confirms the outer-sphere (*anti*) hydroxypalladation mechanism. Our calculations also ratify that the final product formation proceeds through a reductive elimination, assisted by solvent molecules, rather than through β-hydride elimination.

Keywords: isomerization · molecular dynamics · oxidation · reaction mechanisms · Wacker process

Introduction

The Wacker reaction[1] has taken its place in graduate-level inorganic chemistry textbooks as a classic example of homogenous dual-metal catalysis.[2] This reaction comprises the oxidization of olefins into carbonyl compounds by water in the presence of $PdCl_2$ catalyst. Wacker-type oxidation reactions, in their original and modified forms, are still employed today in industrial and laboratory chemistry.[3] Beyond the remarkable chemistry of redox-coupled reactions that are involved in the Wacker process, it highlights various interesting aspects of Pd chemistry and, thus, understanding the molecular details of this reaction is still significant in today's research.[3e] Even after several decades of research on the kinetics and the mechanism of this reaction, various aspects are yet to be resolved.[4] Although there is a consensus on the general features of the reaction mechanism, controversies persist in terms of the stereochemistry of the hydroxypalladation step, which involves nucleophilic attack of water on the olefin, and in terms of the rate-determining step. The origin of the inverse-first-order and inverse-second-order relationships to [H^+] and [Cl^-], respectively, has to be interpreted with a consistent mechanism of this process.

Several kinetic and stereochemical studies have addressed the issue of inner-sphere (*syn*) versus outer-sphere (*anti*) modes of water attack on ethene (see steps **3.1**→**5.1** and **3.2**→**5.2**, Figure 1). Pioneering work along these directions was carried out by Henry; see Ref. [4]) for a review. Initial kinetic studies with deuterated ethene showed no primary kinetic isotope effects, thus indicating that intramolecular hydrogen transfer, that is, the formation of compound **6**, is not rate determining.[5,6] One of the possible mechanisms in-

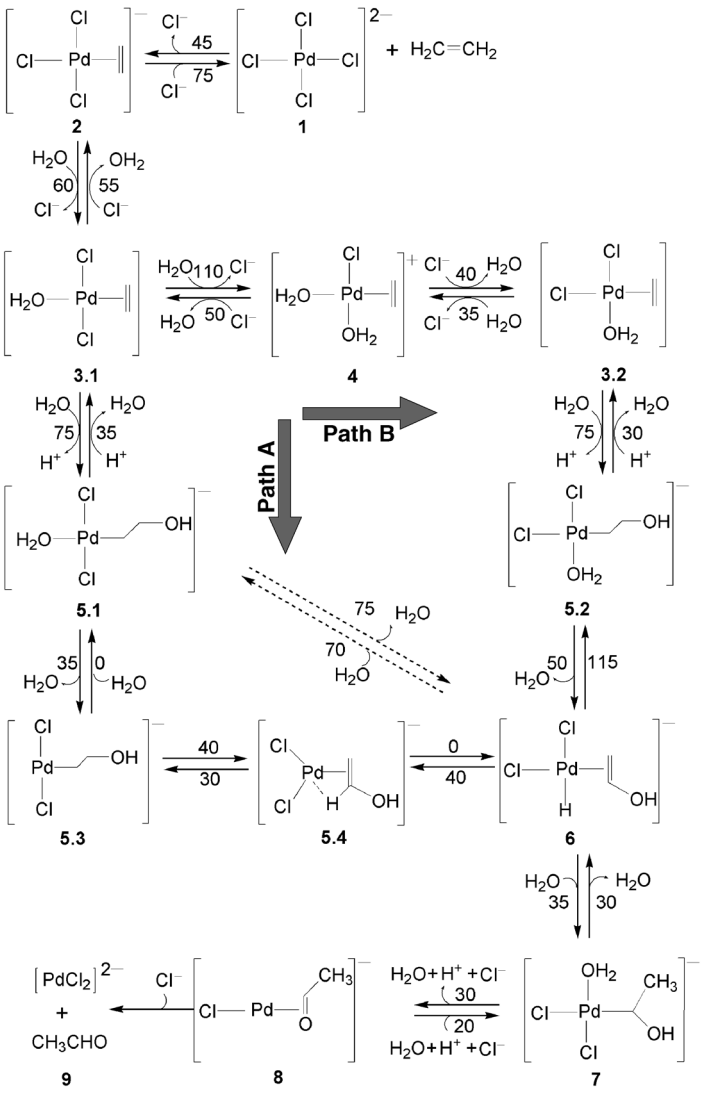

Figure 1. Mechanism of the Wacker oxidation of ethene investigated in this work. Computed free-energy barriers (in kJ mol^{-1}) are indicated above the arrows.

[a] V. Imandi, S. Kunnikuruvan, Dr. N. N. Nair
Department of Chemistry
Indian Institute of Technology Kanpur
Kanpur, 208016 (India)
Fax: (+91) 512-259-7436
E-mail: nnair@iitk.ac.in

Supporting information for this article is available on the WWW under http://dx.doi.org/10.1002/chem.201204342.

volved the formation of a Pd-coordinated hydroxide species from water, in agreement with the experimentally observed first-order proton inhibition, followed by slow hydroxypalladation in a *syn* fashion.[5] Conversely, stereochemical studies of Bäckvall et al.[7] observed an *anti* mode of water attack. First-order proton inhibition in this case was explained by considering that the hydroxypalladation is in equilibrium, followed by some rate-determining steps, which Bäckvall and co-workers interpreted as the elimination of Cl^- from the coordination sphere.[7b] However, this mechanism failed to explain the isotope-scrambling experiments of Henry and co-workers,[8] in which the isomerization of [D_2]allyl-1,1-alcohol into [D_2]allyl-3,3-alcohol during the Wacker process was not observed, which suggested that the hydroxypalladation step does not involve an equilibrium. Stereochemical studies by using substituted olefins indicated that the *syn* route is preferred under low [Cl^-] and [$CuCl_2$] conditions,[9] whereas the *anti* pathway is preferred under high [Cl^-] and [$CuCl_2$] conditions.[7,10]

Most of the previously reported theoretical calculations[11] have focused on the stereochemistry of the hydroxypalladation step and they have consistently predicted the operation of an *anti* mode over a *syn* mode. Some of the quantum-mechanical calculations have also suggested that the intramolecular β-hydrogen transfer step is rate determining. A mechanism in which the simultaneous attack of *cis*-water on the olefin and deprotonation by the solvent was proposed by Goddard and co-workers.[11b] However, only a marginal preference for the *syn* route was noted by these authors. They suggested an isomerization process, subsequent to the hydroxypalladation step, as being the rate-determining step.

The major issue in applying static quantum-chemical calculations to the mechanistic study of the Wacker process is the incorporation of finite solvent effects. In fact, the inclusion of explicit solvent molecules makes these calculations practically difficult. Earlier works by Siegbahn have revealed the crucial importance of incorporating explicit water molecules in modeling this reaction.[11g,h] Accounting for solvent dynamics and, in particular, entropic effects are vital and, to overcome such problems, ab initio molecular dynamics (AIMD) techniques are more appropriate. Recently, Comas-Vives et al.[12] have investigated the mechanistic aspects of the hydroxypalladation step by using AIMD techniques,[13] together with periodic density functional theory (DFT). Interestingly, they observed an important role of the *trans* effect in the Pd–ethene complex in determining its structure, dynamics, and reactivity. The same conclusions were also reached by ourselves[14] through an independent study at about the same time. Importantly, both of these studies observed a preference for an *anti*-mode attack of water over *syn*-mode attack. A more comprehensive analysis of the ligand-exchange mechanisms and their associated equilibria in the catalytic precursor complex have also been reported recently[15] by using the same techniques.

In short, a detailed connection between the rate law and the mechanism has yet to be established. Moreover, a proper justification of the experimentally observed stereochemistry of the hydroxypalladation in substituted olefins, the kinetic isotope effects, and isotope scrambling within the framework of a unified mechanism also remains elusive. Moreover, the rate-determining step needs to be probed.

As a continuation of our efforts to unveil the molecular details of the Wacker oxidation of ethene, herein, we address the detailed mechanism and kinetics of the Wacker process under low [Cl^-], low [$CuCl_2$], and ambient aqueous conditions. We show that the mechanism established herein, which involves an *anti*-mode attack of water, complies well with the experimentally estimated free-energy barrier and the observed rate law at low [Cl^-].

We began our investigation with catalyst precursor **1** and continued through to the final product formation (Figure 1). The catalyst model used herein assumes no direct involvement of $CuCl_2$ or the formation of Pd–Cu heterometallic complexes. This assumption is reasonable at low [$CuCl_2$] under aqueous conditions and is supported by the fact that the [$CuCl_2$] term is absent in the rate law of the Wacker process. Experimentally, oxo-bridged Pd–Cu complexes have only been isolated under non-aqueous conditions.[16] Cl-bridged dinuclear Pd complex structure for the catalyst has also been a matter of debate in the literature.[17] At high or moderate [Pd^{II}], under non-aqueous conditions or in solvent mixtures with water, the formation of a dimer seems to occur, which explains the different rate expression that is observed under these conditions. Recently, this result has been further confirmed by MS (ESI) studies.[18] Thus, the mono-Pd catalyst used in the current work, corresponds to an experiment in water solvent at low [Cu^{II}], [Pd^{II}], and [Cl^-].

To simulate the chemical reactions, we employed metadynamics techniques,[19] together with AIMD, based on periodic DFT. Metadynamics is a powerful technique to simulate chemical reactions within the short timescale that is accessible to AIMD and to elicit the reaction pathways and associated free-energy changes (for selected reviews, see Ref. [20]). In our calculations, the accuracy of the free-energy estimates is $\pm 5\ kJ\,mol^{-1}$, owing to the metadynamics simulation procedures that are followed, and about $1\ kJ\,mol^{-1}$, owing to the employed PBE density functional (with respect to a more-accurate hybrid meta-GGA functional; see the Supporting Information). All of the reconstructed free-energy surfaces that are used for the estimation of free energies are also available in the Supporting Information.

Results and Discussion

The **1**→**2**→**3.1** reaction involves ligand-exchange processes in a stepwise manner. The *trans* effect of a Pd–olefin complex is found to favor the formation of structure **3.1**, in the same way as observed in simulations at high [Cl^-][14] and low [Cl^-].[12,15] In all of these cases, the ligands approach from the solution and coordinate with the Pd complex in the axial position, in tandem with the release of the *trans*

ligand. Surprisingly, the *trans* effect of the complex was neglected in the earlier work by Henry.[5] The barriers for the steps up to the formation of structure **3.1** are in reasonably good agreement with the results of previous AIMD simulations.[12,15] The ligand-exchange processes follow an associative pathway, that is, the incoming ligand (i.e., water) approaches in an axial manner towards the square-planar complex, thereby forming a trigonal-bipyramidal intermediate, and subsequently loses the *trans*-Cl group (Figure 2a–c).

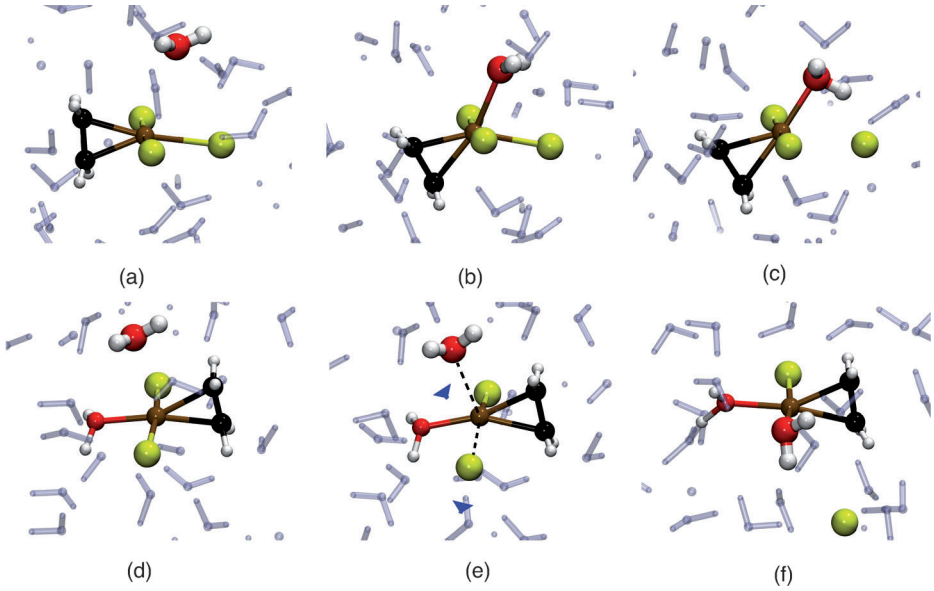

Figure 2. Snapshots from the reactive trajectories of simulated steps **2**→**3.1** (a–c) and **3.1**→**4** (d–f): a) Axial approach of a water molecule to square-planar complex **2**; b) trigonal-bipyramidal transition-state structure; c) elimination of a *trans*-Cl ligand; d) axial approach of a water molecule to complex **3.1**; e) T-shaped transition-state structure (arrows indicate the motion of the approaching water molecule and the exchanging *cis*-Cl ligand to form structure (f)). Color scheme: Pd brown, Cl yellow, C black, O red, H white, solvent water molecules gray sticks.

This mechanism is anticipated for d^8 square-planar complexes with strong *trans*-directing ligands.[21]

However, the difference in Gibbs free energy (ΔG) between structures **1** and **2**, as estimated by experiments (-7 kJ mol^{-1})[5] is much lower in magnitude than the computed Helmholtz free-energy difference (ΔF) between structures **1** and **2** (-30 kJ mol^{-1}). This variance could be attributed to the error in the free-energy estimates, the differences in the ensemble that is used, or to finite size effects. In the previous AIMD studies at low [Cl$^-$],[15] ΔF was estimated to be $+20$ kJ mol^{-1}.

We found that the reaction **3.1**→**7** could proceed through two different pathways, that is, **3.1**→**5.1**→**6**→**7** (path A) and **3.1**→**5.2**→**6**→**7** (path B; Figure 1). These two pathways differ in the position of the Cl$^-$ ligand when it undergoes the hydroxypalladation reaction. As will be clear from the detailed discussion below, the positions of Cl$^-$ ligands have a significant effect on the overall reaction kinetics.

At low [Cl$^-$], reaction **3.1**→**5.1**, that is, the hydroxypalladation step, has a free energy barrier of 75 kJ mol^{-1}. Most importantly, the barrier for the reverse process, **5.1**→**3.1**, only has a barrier of 35 kJ mol^{-1}. The forward free-energy barrier is in quantitative agreement with previous calculations[12,14] by using similar techniques. The hydroxypalladation step proceeds through an *anti* mode of attack, which is the only possibility for compound **3.1**, in which both *cis* positions are occupied by Cl$^-$ ions. In this case, the deprotonation of the coordinating water molecule occurs concurrently with C–O bond formation. As reported previously,[14] the slipping motion[22] of the olefin occurs prior to the water attack, thus resulting in a transient η^1-coordination.

The next step, that is, **5.1**→**6**, involves a β-hydrogen elimination. Not many theoretical investigations have focused on this step and, thus, a detailed analysis of the mechanism is reported herein. It is clear that, during the reaction, a H atom migrates from the β-C atom to the Pd center and takes over the *cis* position, which is preoccupied by Cl$^-$ ions (in structure **5.1**). Thus, an isomerization, by the *cis*-to-*trans* rotation of a Cl$^-$ ligand, is essential, either prior to or in conjunction with the β-hydrogen transfer. However, the dissociation of a *cis*-Cl$^-$ ligand would require a higher free energy than isomerization, which will be discussed below. We found that the reaction involved an initial discharge of the *trans*-water molecule (thus forming structure **5.3**), followed by isomerization prior to β-hydrogen transfer (Figure 3). Most significantly, the hydrogen transfer occurs spontaneously after the isomerization. Thus, the process with the highest free-energy requirement on going from **5.1**→**6** is the isomerization step and not the *trans*-water discharge or the H shift. We observed several *trans*-water exchanges in the simulations, but never a β-hydrogen transfer that preceded the isomerization step, thus supporting this conclusion.

Cis-to-*trans* rotation of a Cl$^-$ ligand in structure **5.3** occurs through a narrowing of the Cl-Pd-Cl angle along the bending mode of its vibration. In the transition-state structure, all of the C, Pd, and Cl atoms lie almost in a plane. One of the bonding orbitals (the eighth state below the HOMO, HOMO−8) of transient structure **5.4** has weak Pd–H and partial C–C π-bond formation (Figure 3g). The weak Pd–H bond formation in structure **5.4** can also justify the presence of secondary isotope effects in the Wacker oxidation of ethene. Interestingly, the LUMO of this structure has substantial contributions from C–C (π), Pd (d), and H (s) orbitals. This result explains the subsequent spontaneous reaction, in which hydrogen atom transfers onto the Pd center,

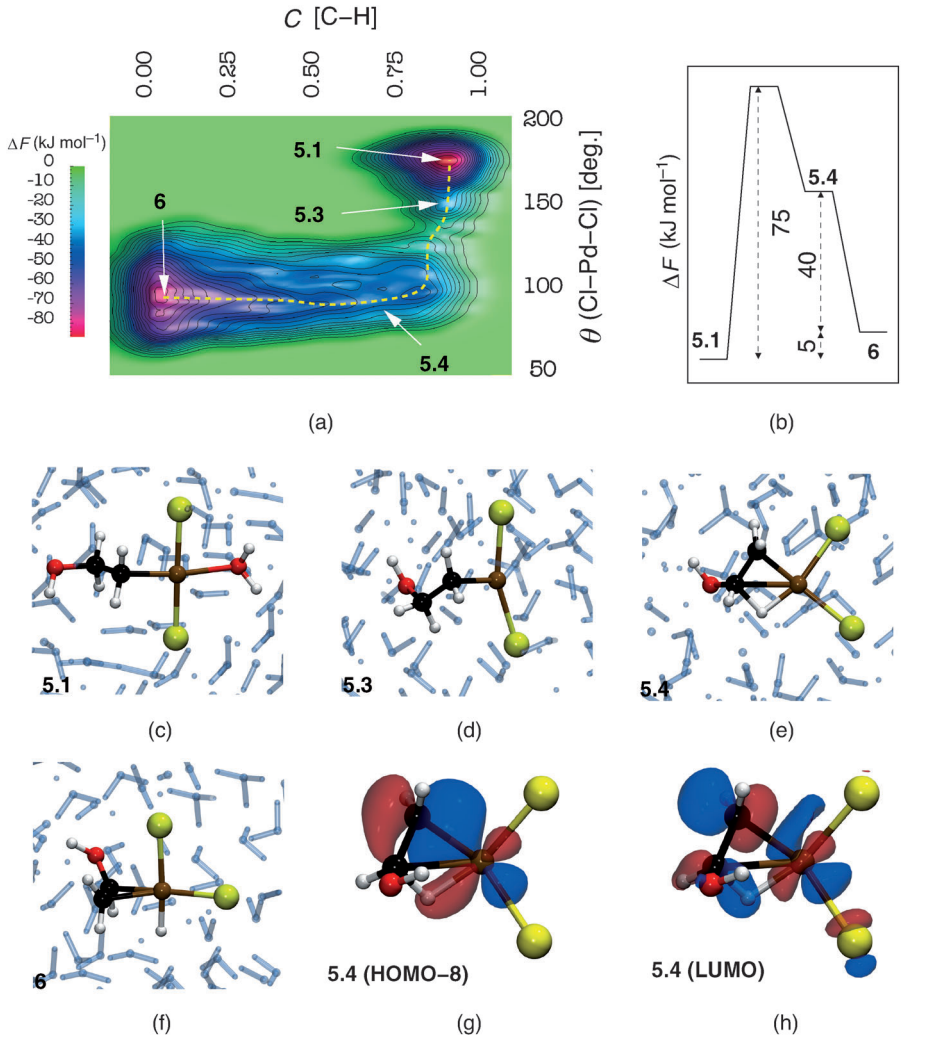

Figure 3. Free-energy surface (a) and free-energy profile (b) of step **6**→**5.1**; the minimum-energy pathway that connects structures **6** and **5.1** is indicated by dotted lines. Relevant snapshots from the simulation are shown in (c–f). Natural localized molecular orbitals of the HOMO−8 and LUMO states of transient structure **5.4** are shown in (g) and (h), respectively (isovalues ±0.04 *e*).

thus resulting in compound **6**. We also observed that the Pd−Cl bonding orbitals are much lower in energy than the HOMO (HOMO−10). Therefore, it is clear that the isomerization step is energetically preferred over Pd−Cl dissociation.

In an independent simulation, in which we sampled the Cl-Pd-Cl angle and the Pd coordination number but not explicitly the collective coordinates that described the β-hydrogen transfer, the same mechanism was observed, that is, the hydrogen transfer occurred spontaneously subsequent to the isomerization step. To further affirm this conclusion, we carried out a simulation of the reverse process, that is, **6**→**5.1**. The reconstructed free-energy surface (Figure 3) distinctly shows the absence of a free-energy barrier on going from **5.4**→**6** and that the rate-determining step in **5.1**→**6** only involves isomerization and no β-hydrogen transfer.

The barrier for step **5.1**→**6** (75 kJ mol^{-1}) is much higher than that for **5.1**→**3.1**, thus implying the existence of the equilibrium **3.1**⇌**5.1** (Figure 5). The presence of this equilibrium is crucial in interpreting the experimental rate law, which will be discussed below.

An alternative route to structure **6** proceeds through structure **5.2**. Thus, next, we looked at the formation of structure **5.2** from structure **3.1**, which could circumvent the rate-determining isomerization step. In structure **3.1**, the ligand exchange of *cis*-Cl$^-$ with bulk water (**3.1**→**4**) requires about 110 kJ mol^{-1}, which is in qualitative agreement with previous calculations.[14] The *trans* effect of the Pd−ethene complex favors ligand exchange at the *trans* position;[12,14] however, *cis* ligand exchange is a slow process. On the other hand, the attack of Cl$^-$ ions at the *trans* position in structure **4** (**4**→**3.2**) and its reverse process (**3.2**→**4**) are relatively fast ($\Delta F^{\neq}$ = 40 and 35 kJ mol^{-1}, respectively), both boosted by the *trans* effect. With the approach of a ligand from the axial position, a trigonal-bipyramidal structure (as in Figure 2b) is always formed. In this structure, the *cis* ligands lie in an axial position, thereby forming strong σ bonds with the d_z^2 orbital. Thus, the weak equatorial ligands are preferably exchanged, as shown in Figure 2a–c. During the *cis* ligand exchange along **3.1**→**4**, we didn't observe the formation of a trigonal-bipyramidal structure. Instead, the *cis* ligand exchange follows a dissociative-type mechanism, in which a T-type intermediate is formed by the dissociation of a *cis*-Cl ligand from the coordination sphere, followed by the attack of an external water molecule (Figure 2e).

The resulting structure (**3.2**) undergoes a hydroxypalladation reaction, thereby forming structure **5.2**. The mechanism of this step is certainly of importance because of the controversy that surrounds the stereochemistry of the hydroxypalladation. The simulation procedure that we followed was such that, of the two possibilities of water attack, that is, *anti* versus *syn*, only the one with the lowest free-energy barrier was sampled. The free-energy barrier for step **3.2**→**5.2** was 75 kJ mol^{-1}, the same as that for **3.1**→**5.1**, and it proceeded through an *anti* mode of water addition. This result is in quantitative and qualitative agreement with previous AIMD calculations,[12,14] in which the *anti* mode was found to be preferred over the *syn* mode. Although, we didn't per-

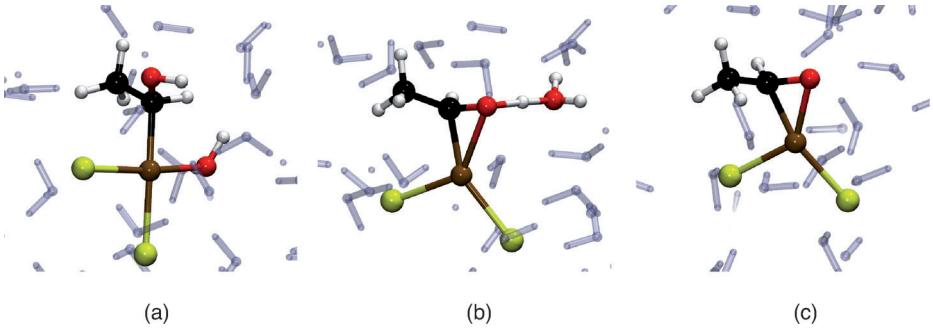

Figure 4. Snapshots from the metadynamics simulation of step **7**→**8**: a) Starting structure **7**; b) transient structure, in which a proton is transferred from the hydroxy group to a solvent water molecule; c) product structure **8**. In (b) and (c), the Pd, O, α-C, and Cl atoms lie in a plane.

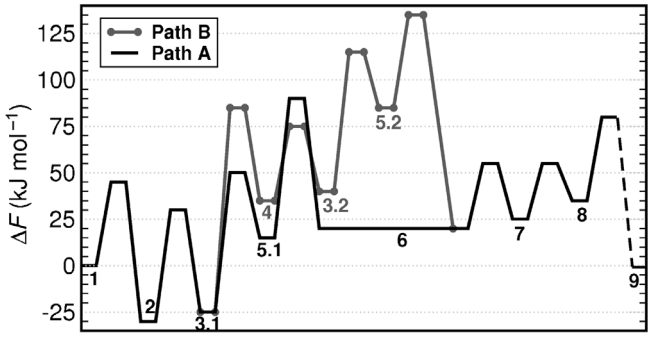

Figure 5. Free-energy profiles based on the free-energy barriers along paths **1**→**5.1**→**9** (A) and **1**→**5.2**→**9** (B). The reverse barrier for step **9**→**8** was not computed and, thus, is indicated by a dotted line.

form simulations to estimate the free-energy barrier for the *syn* mode, we can conclude from our results that it should be associated with a higher free-energy barrier than the *anti* mode. The *syn* mode of hydroxypalladation at low [Cl^-] was simulated by Comas-Vives et al.,[12] who estimated the free-energy barrier to be about 200 kJ mol^{-1}.

The reverse reaction, that is, **5.2**→**3.2**, only has to overcome a barrier of 30 kJ mol^{-1}, which is again consistent with step **5.1**→**3.1**. The hydroxylated product (**5.2**) then proceeds through a β-hydrogen elimination to form compound **6**. In this step, the dissociation of *cis* water from the coordination sphere of Pd is the rate-determining step and subsequent β-hydrogen transfer takes place. The free-energy barrier for the former process is only 50 kJ mol^{-1}, which is 25 kJ mol^{-1} lower than that for the reaction **5.1**→**6**.

Attempts to simulate the reaction **6**→**5.2** always resulted in the formation of structure **5.1**, thus hinting a much higher barrier for this process. However, this reaction can be computed, based on the relative energies of structures **5.2** and **6** with respect to **3.1**, and is about 115 kJ mol^{-1}.

In the subsequent step, structure **6** rearranges into structure **7** through a hydrogen transfer from the Pd center onto the α-carbon of the hydroxylated olefin. After the hydrogen transfer, the freed *cis* position is occupied by a solvent water molecule. The barrier for the entire process is 35 kJ mol^{-1}. The reverse process consists of *cis* ligand dissociation, followed by hydrogen transfer from the α-carbon atom onto Pd. While simulating the reverse process, we observed initial *cis*-Cl dissociation, followed by hydrogen transfer. A lower free-energy barrier for the *cis* ligand exchange in structure **7** compared to that in structure **3.1** can be explained by the strong *trans* effect of ethene in structure **3.1** compared to a weak *trans* effect of the (CH_3)–CH(OH) moiety in structure **7**.

The following step, **7**→**8**, involves the release of a proton from the OH group of the coordinated alkyl alcohol (**7**), thus resulting in a coordinated acetaldehyde species. This step is not believed to involve a β-hydrogen elimination,[7b,23] but rather to proceed through a deprotonation from the OH group to either the Cl^- ion[11a] or a solvent water molecule.[11e] We carried out this reaction in such a manner that, of these different routes, only the one with the minimum free-energy barrier would be sampled. We found that deprotonation of the OH group occurred to a solvent water molecule, but not to Cl^- or to Pd (i.e., β-hydrogen elimination), in agreement with the results reported in Ref. [11e] (Figure 4). This deprotonation is consistent with the O–Pd bond formation (Figure 4b). In the product (**8**), the acetaldehyde is π-complexed with the Pd^0 center. The free-energy barrier for the forward (**7**→**8**) and reverse processes (**8**→**7**) are 30 kJ mol^{-1} and 20 kJ mol^{-1}, respectively.

The final product-formation step, that is, **8**→**9**, involves the reductive elimination of the π-complexed acetaldehyde. We simulated the reaction **8**→**9** and the associated free-energy barrier was estimated to be 45 kJ mol^{-1}.

Now, considering the overall reaction (**1**→**9**), there are two possible mechanisms: Path A, which proceeds through structure **5.1**, and path B, which proceeds through structure **5.2** (Figure 5). Along path A, hydroxypalladation is not the rate-determining step. The bottleneck is the isomerization by *cis*-to-*trans* ligand rotation (**5.1**→**6**). For step **5.1**→**6**, β-hydrogen exchange occurs in a spontaneous manner, subsequent to the isomerization, and, thus, primary kinetic isotope effects are not expected, in agreement with the experimental data.[5,6]

Having obtained the forward and reverse barriers, we can derive the rate expression for the entire process. Along path A, the rate law has the form given in Equation (1), where $\{k_i\}$ are rate constants and k_{eff} is the effective rate constant.

$$-\frac{d[CH_2CH_2]}{dt} = \frac{k_\alpha[PdCl_4^{2-}][CH_2CH_2]}{[Cl^-]^2(k_\beta + k_\gamma[H^+] + k_\delta[H^+]^2) + k_\omega[Cl^-] + k_\varepsilon} \approx \frac{k_{eff}[PdCl_4^{2-}][CH_2CH_2]}{[H^+][Cl^-]^2} \quad (1)$$

This simplification of the rate expression is achieved by considering that $[Cl^-] \ll [H_2O]$ and by comparing the values of the rate constants (evaluated by using the transition-state theory; for a detailed derivation, see the Supporting Information). This expression is in complete agreement with the experimentally observed rate law at low $[Cl^-]$.[5]

Having derived this expression, we can now dissect the origins of the H^+ and Cl^- inhibition. The presence of the proton-inhibition term is contributed to by the hydroxypalladation step and the second-order chloride inhibition is due to the ligand-exchange steps along the process **1**→**3.1**. Simplification of the rate expression (as shown above) takes advantage of the fact that the rate constant for step **5.1**→**6** is negligible compared to that of **5.1**→**3.1**, or, in other words, the existence of the equilibrium **3.1**⇌**5.1** and a subsequent slow step are crucial for obtaining the above rate law. Earlier theoretical attempts at deriving the rate law by using quantum-chemical calculations failed to explain the second-order Cl^- inhibition.[11c] By using the transition-state theory, the free-energy barrier that corresponds to the effective rate constant (k_{eff}) is 90 kJ mol^{-1}, which is in excellent quantitative agreement with the experimental data (see the Supporting Information). However, this agreement is surprising, owing to the associated errors that are present in our free-energy estimates (as discussed above).

From Figure 5, it is clear that path B is slower than path A. In fact, path B also gives the same rate law, but has an effective barrier of about 135 kJ mol^{-1} (see the Supporting Information). Thus, this pathway is ruled out for ethene oxidation at low $[Cl^-]$.

Conclusions

Our calculations, by employing ab initio molecular-dynamics simulation techniques, have resolved the mechanistic and kinetic details of the Wacker oxidation of ethene at low $[Cl^-]$, starting from the ligand-exchange steps that involve the mononuclear Pd^{II} catalytic precursor through to the final product (acetaldehyde) formation.

We scrutinized a new rate-determining step, which involves isomerization through a *cis*-to-*trans* ligand rotation. This isomerization occurs in the tri-coordinated intermediate that is formed after the release of the *trans* water. The rate-determining step is succeeded by a hydroxypalladation step, but prior to β-hydrogen elimination. The latter step occurs spontaneously after the isomerization, through a transient species that has weak a Pd–H bond, thus explaining the absence of any primary isotope effects and the presence of secondary isotope effects.

This work establishes the existence of an equilibrium hydroxypalladation step, unlike the earlier mechanistic proposals by Henry and co-workers. Our findings profoundly agree with the mechanistic picture put forward by Bäckvall et al.,[7] except for the proposed slow step.

We show that, for ethene, the question of *anti*- versus *syn*-type hydroxypalladation is immaterial because the preferred reaction pathway does not involve any *cis* ligand exchange and, thus, *anti*-type attack is the only possibility. Wacker oxidation through a *cis* ligand exchange (path B) is much slower than the route that does not involve the *cis* exchange (path A). The *cis* ligand exchange follows a dissociative mechanism, with the formation of a T-shaped intermediate. However, a trigonal-bipyramidal structure is formed when a water molecule approaches the complex in an axial manner, facilitating *trans* ligand exchange. Even in path B, the *anti* mode of hydroxypalladation is preferred, in agreement with the previous theoretical work with AIMD. We also found that the final product formation did not proceed through β-hydride elimination, but rather through a proton transfer to the solvent, followed by reductive elimination.

For both path A and path B, the rate expressions show an inverse-first-order dependence on $[H^+]$ and an inverse-second-order dependence on $[Cl^-]$. The rate-determining step in path A is the isomerization step, whereas, in path B, it is the dissociation of the Pd–OH_2 bond. Still, these paths show the same rate law, because, in both cases, the rate-determining step occurs after the hydroxypalladation step. Herein, we have confirmed that, for a mechanism that involves an equilibrium hydroxypalladation step, the rate law of the entire reaction process is in full agreement with the experimentally observed rate law and that it is not essential to have a rate-determining hydroxypalladation step, as proposed by Henry.[5] It is interesting to note the origin of $[H^+]$ and $[Cl^-]$ inhibition terms in the rate law, based on this proposed mechanism. The first-order proton inhibition is a result of the equilibrium hydroxypalladation step and the second-order chloride inhibition is due to the Cl^- ligand-exchange steps that occur prior to the hydroxypalladation step. The effective reaction free-energy barrier, based on an effective rate constant, is in qualitative agreement with the experimentally determined value.

Although our proposed mechanism could explain many of the crucial experimental observations, it is unable to clarify the isotope-scrambling experiments of Henry and co-workers.[8] The existence of the equilibrium **3.1**⇌**5.1** could have resulted in the formation of $[D_2]$allyl-3,3-alcohol during the Wacker oxidation of $[D_2]$allyl-1,1-alcohol, but was only observed in trace amounts. The only way that this result can be explained is that the mechanism of ethene oxidation is different than allyl alcohol, although the observed rate laws are identical. However, an earlier report on the oxidation of allyl alcohol by using static quantum-chemical calculations didn't show a different mechanistic route.[11f] It is likely that the dπ–pπ bonding between Pd and the olefin is weaker compared to ethylene, owing to the electronic effects of the CH_2OH moiety. Thus, the crucial *trans* effect is weaker in allyl alcohol, which may affect the reaction mechanism and kinetics. Alternative reaction pathways may also be active in this case, because alcoholic oxygen atoms can coordinate with Pd or the reaction can proceed through an intramolecular hydroxypalladation step.[24]

The concerns regarding the dependence of the reaction mechanism on the structure of the olefin will be addressed

in future work, which is also crucial for interpreting the stereochemical studies that have demonstrated a *syn* mode of water attack. At the same time, the effects of [Cl^-], [Pd^{II}], and [Cu^{II}] on the reaction, including the formation of dinuclear complexes, also need to be probed. We believe that the details of the reaction mechanism and kinetics reported herein will lay a platform for future research along these directions.

Experimental Section

Periodic DFT calculations were carried out by using the plane-wave basis set and the PBE[25] exchange-correlation functional, as available in the CPMD[26] simulation package. Only valence electrons were treated explicitly, whereas the interactions between the core and the valence electrons were accounted for by ultrasoft pseudopotentials. We employed a plane-wave cutoff of 30 Ry. Car–Parrinello simulations[13] were performed with a fictitious orbital mass of 700 and a time step of 0.145 fs. An extended Lagrangian metadynamics scheme[19] was employed to simulate the chemical reactions. The reaction in bulk water was modeled by using 29 water molecules, together with complex **1** in a periodic supercell of size 10.0 Å × 10.0 Å × 10.0 Å, roughly reproducing the density of water at 300 K. Natural localized molecular orbitals[27] of structure **5.4** were computed for its gas-phase-optimized structure by using the Gaussian 09[28] suite of programs with the 6-31G+** basis set by using the PBE functional. More technical details regarding the simulation set-up and the collective coordinates that are used in the metadynamics simulations are available in the Supporting Information.

Acknowledgements

The authors thank the Department of Chemistry, IIT Kanpur for the use of the ChemFIST computational facility and the CSIR, India, for funding the project. V.I. and S.K. thank the UGC and IIT Kanpur for their Ph.D. fellowships.

[1] J. Smidt, W. Hafner, R. Jira, J. Sedlmeier, R. Sieber, R. Rüttinger, H. Kojer, *Angew. Chem.* **1959**, *71*, 176–182.
[2] a) F. A. Cotton, C. A. Murillo, M. Bochmann, *Advanced Inorganic Chemistry, 6th ed.*, Wiley-Interscience, New York, **1999**; b) G. Rothenberg, *Catalysis: Concepts and Green Applications*, Wiley-VCH, Weinheim, **2008**.
[3] a) J. M. Takacs, X. Jiang, *Curr. Org. Chem.* **2003**, *7*, 369–396; b) J. Tsuji, *Synthesis* **1984**, 369–384; c) A. Heumann, M. Ré-glier, *Tetrahedron* **1996**, *52*, 9289–9346; d) C. N. Cornell, M. S. Sigman, *Inorg. Chem.* **2007**, *46*, 1903–1909; e) M. S. Sigman, E. W. Werner, *Acc. Chem. Res.* **2012**, *45*, 874–884.
[4] J. A. Keith, P. M. Henry, *Angew. Chem.* **2009**, *121*, 9200–9212; *Angew. Chem. Int. Ed.* **2009**, *48*, 9038–9049.
[5] P. M. Henry, *J. Am. Chem. Soc.* **1964**, *86*, 3246–3250.
[6] a) P. M. Henry, *J. Org. Chem.* **1973**, *38*, 2415–2416; b) M. Kosaki, M. Isemura, Y. Kitaura, S. Shinoda, Y. Saito, *J. Mol. Catal.* **1977**, *2*, 351–359; c) Y. Saito, S. Shinoda, *J. Mol. Catal.* **1980**, *9*, 461–464.
[7] a) J. E. Bäckvall, B. Åkermark, S. O. Ljunggren, *J. Chem. Soc. Chem. Commun.* **1977**, 264–265; b) J. E. Bäckvall, B. Åkermark, S. O. Ljunggren, *J. Am. Chem. Soc.* **1979**, *101*, 2411–2416.
[8] M. K. Wan, K. Zaw, P. M. Henry, *Organometallics* **1988**, *7*, 1677–1683.
[9] J. W. Francis, P. M. Henry, *Organometallics* **1991**, *10*, 3498–3503.
[10] a) N. Gregor, K. Zaw, P. M. Henry, *Organometallics* **1984**, *3*, 1251–1256; b) J. W. Francis, P. M. Henry, *Organometallics* **1992**, *11*, 2832–2836.
[11] For a review and further references, see Ref. [4]; a) J. A. Keith, J. Oxgaard, W. A. Goddard III, *J. Am. Chem. Soc.* **2006**, *128*, 3132–3133; b) J. A. Keith, R. J. Nielsen, J. Oxgaard, W. A. Goddard III, *J. Am. Chem. Soc.* **2007**, *129*, 12342–12343; c) S. A. Beyramabadi, H. Eshtiagh-Hosseini, M. R. Housaindokht, A. Morsali, *Organometallics* **2008**, *27*, 72–79; d) B. J. Anderson, J. A. Keith, M. S. Sigman, *J. Am. Chem. Soc.* **2010**, *132*, 11872–11874; e) S. A. Beyramabadi, H. Eshtiagh-Hosseini, M. R. Housaindokht, A. Morsali, *J. Mol. Struct. THEOCHEM* **2009**, *903*, 108–114; f) J. A. Keith, R. J. Nielsen, J. Oxgaard, W. A. Goddard III, *Organometallics* **2009**, *28*, 1618–1619; g) E. M. Siegbahn, *J. Am. Chem. Soc.* **1995**, *117*, 5409–5410; h) E. M. Siegbahn, *J. Phys. Chem.* **1996**, *100*, 14672–14680.
[12] A. Comas-Vives, A. Stirling, A. Lledós, G. Ujaque, *Chem. Eur. J.* **2010**, *16*, 8738–8747.
[13] D. Marx, J. Hutter, *Ab Initio Molecular Dynamics: Basic Theory and Advanced Methods*, Cambridge University Press, Cambridge, **2009**.
[14] N. N. Nair, *J. Phys. Chem. B* **2011**, *115*, 2312–2321.
[15] G. Kovács, A. Stirling, A. Lledós, G. Ujaque, *Chem. Eur. J.* **2012**, *18*, 5612–5619.
[16] a) T. Hosokawa, M. Takano, S.-I. Murashashi, *J. Am. Chem. Soc.* **1996**, *118*, 3990–3991; b) T. Hosokawa, M. Takano, S. I. Murashashi, *J. Organomet. Chem.* **1998**, *551*, 387–389; c) Y. Kawamura, Y. Kawano, T. Matsuda, Y. Ishitobi, T. Hosokawa, *J. Org. Chem.* **2009**, *74*, 3048–3053.
[17] a) P. M. Henry, *J. Am. Chem. Soc.* **1972**, *94*, 4437; b) I. I. Moiseev, O. G. Levanda, M. N. Vargaftik, *J. Am. Chem. Soc.* **1974**, *96*, 1003–1007.
[18] D. Harakat, J. Muzart, J. L. Bras, *RSC Adv.* **2012**, *2*, 3094.
[19] M. Iannuzzi, A. Laio, M. Parrinello, *Phys. Rev. Lett.* **2003**, *90*, 238302.
[20] a) B. Ensing, M. D. Vivo, Z. W. Liu, P. Moore, M. L. Klein, *Acc. Chem. Res.* **2006**, *39*, 73; b) A. Laio, F. L. Gervasio, *Rep. Prog. Phys.* **2008**, *71*, 126601; c) A. Barducci, M. Bonomi, M. Parrinello, *WIREs Comput. Mol. Sci.* **2011**, *1*, 826–843.
[21] G. K. Anderson, R. Cross, *J. Chem. Soc. Rev.* **1980**, *9*, 185–215.
[22] O. Eisenstein, R. Hoffmann, *J. Am. Chem. Soc.* **1981**, *103*, 4308–4320.
[23] R. F. Heck, *Hercules Chem.* **1968**, *57*, 12.
[24] T. Hosokawa, S. I. Murahashi, *Acc. Chem. Res.* **1990**, *23*, 49–54.
[25] J. P. Perdew, K. Burke, M. Ernzerhof, *Phys. Rev. Lett.* **1996**, *77*, 3865.
[26] CPMD, version 13.3, IBMCorp **1990–2012**,MPI für Festkörper-forschung Stuttgart **1997–2001**; also see http://www.cpmd.org.
[27] A. E. Reed, F. Weinhold, *J. Chem. Phys.* **1985**, *83*, 1736.
[28] Gaussian 09 (Revision B.01), M. J. Frisch, G. W. Trucks, H. B. Schlegel, G. E. Scuseria, M. A. Robb, J. R. Cheeseman, G. Scalmani, V. Barone, B. Mennucci, G. A. Petersson, H. Nakatsuji, M. Caricato, X. Li, H. P. Hratchian, A. F. Izmaylov, J. Bloino, G. Zheng, J. L. Sonnenberg, M. Hada, M. Ehara, K. Toyota, R. Fukuda, J. Hasegawa, M. Ishida, T. Nakajima, Y. Honda, O. Kitao, H. Nakai, T. Vreven, J. A. Montgomery, Jr., J. E. Peralta, F. Ogliaro, M. Bearpark, J. J. Heyd, E. Brothers, K. N. Kudin, V. N. Staroverov, R. Kobayashi, J. Normand, K. Raghavachari, A. Rendell, J. C. Burant, S. S. Iyengar, J. Tomasi, M. Cossi, N. Rega, J. M. Millam, M. Klene, J. E. Knox, J. B. Cross, V. Bakken, C. Adamo, J. Jaramillo, R. Gomperts, R. E. Stratmann, O. Yazyev, A. J. Austin, R. Cammi, C. Pomelli, J. W. Ochterski, R. L. Martin, K. Morokuma, V. G. Zakrzewski, G. A. Voth, P. Salvador, J. J. Dannenberg, S. Dapprich, A. D. Daniels, Ö. Farkas, J. B. Foresman, J. V. Ortiz, J. Cioslowski, D. J. Fox, Gaussian, Inc., Wallingford CT, **2010**; see also http://www.gaussian.com/..

Received: December 5, 2012
Published online: March 13, 2013

